

Vojtěch BĚTÁK*, Jiří FÜRST**

DEVELOPMENT OF TWO WAY COUPLED EULER – EULER DROPLETS MODEL

VÝVOJ DVOJCESTNĚ SVÁZANÉHO EULER – EULER MODELU PRO POHYB KAPEK

Abstract

A development of droplet solver for 3D complex geometry is described in this work. This solver is composed of solvers for turbulent flow field and droplets. This code is based on the finite volume method. An open source CFD code OpenFOAM was chosen for its first implementation and first results are shown.

Abstrakt

V této práci je popsán vývoj modelu pro řešení pohybu kapek na komplexních 3D geometriích. Tento řešič je složen z řešiče turbulentního proudového pole a z řešiče pro pohyb kapek. Tento kód je založen na metodě konečných objemů. Pro první implementaci tohoto modelu byl vybrán open source CFD kód OpenFOAM a jsou ukázány první výsledky tohoto modelu.

1 INTRODUCTION

For many problems in fluid mechanics it's necessary to solve a motion of cloud particles (e.g. a flow of steam with evaporation or condensation, a combustion of fuel or a prediction of ice accretion on airplanes). There are two main approaches how to simulate motion of cloud. The first one is a Lagrangian approach which is better and more accurate for cloud with small number of particles. The second one is an Eulerian approach which is better and faster for cloud with high number of particles. The target area of this code is simulation of ice accretion on 3D complex geometry. This code will be composed of the solver for incompressible turbulent flow field and of the solver for Eulerian droplet model. This both model will be coupled.

* Ing., Czech Technical University, Faculty of Mechanical Engineering, Department of Technical Mathematics, Karlovo nám 13, Praha 2, betakvojtech@gmail.com

** doc.,Ing., Ph.D., Czech Technical University, Faculty of Mechanical Engineering, Department of Technical Mathematics, Karlovo nám 13, Praha 2

2 MODEL OF TURBULENT FLOW FIELD

The flow field is considered as incompressible Reynolds averaged Navier – Stokes equations (RANS). EARSM model [8] and Spalart – Allmaras model [1] of turbulent field was chosen. The RANS-EARSM model is described by this system of PDE's.

$$\frac{\partial u_i}{\partial x_i} = 0, \quad (1)$$

$$\frac{\partial u_i}{\partial t} + \frac{\partial u_i u_j}{\partial x_j} = -\frac{\partial \tilde{p}}{\partial x_i} + \frac{\partial}{\partial x_j} \left(\nu \frac{\partial u_i}{\partial x_j} \right) - \overline{u_i' u_j'} + \zeta \cdot f_i, \quad (2)$$

$$\frac{\partial k}{\partial t} + \frac{\partial k u_j}{\partial x_j} = P - \beta^* k \omega + \frac{\partial}{\partial x_j} \left[(\nu + \nu_t \sigma_k) \frac{\partial k}{\partial x_j} \right], \quad (3)$$

$$\frac{\partial \omega}{\partial t} + \frac{\partial \omega u_j}{\partial x_j} = \gamma \frac{\omega}{k} P - \beta \omega^2 + \frac{\partial}{\partial x_j} \left[(\nu + \nu_t \sigma_\omega) \frac{\partial \omega}{\partial x_j} \right] + \frac{\sigma_d}{\omega} \max \left(\frac{\partial k}{\partial x_j} \frac{\partial \omega}{\partial x_j}, 0 \right). \quad (4)$$

The model constant and function are defined as follows

$$\Gamma_1 = \frac{\sqrt{k}}{\beta^* \omega d}, \quad \Gamma_2 = \frac{500\nu}{\omega d^2}, \quad \Gamma_3 = \frac{20k}{\max \left[\frac{d^2}{\omega} \frac{\partial k}{\partial x_j} \frac{\partial \omega}{\partial x_j}, 200k_\infty \right]}, \quad (5)$$

$$\Gamma = \min[\max(\Gamma_1, \Gamma_2), \Gamma_3], \quad f_{mix} = \tanh(C_{mix} \Gamma^4), \quad (6)$$

$$\omega_w = \frac{u_\tau^2}{\nu} S_R, \quad k_{smin}^+ = \min[2.4(y_1^+)^{0.85}, 8], \quad S_R = \begin{cases} [50 / \max(k_s^+, k_{smin}^+)]^2 & k_s^+ < 25 \\ 100 / k_s^+ & k_s^+ \geq 25 \end{cases}, \quad (7)$$

$$\varphi = f_{mix} \varphi_1 + (1 - f_{mix}) \varphi_2, \quad (8)$$

Tab 1: Coefficients of EARSM turbulence model

	γ	β	σ_k	σ_ω	σ_d
Set 1	0.518	0.0747	1.1	0.53	1
Set 2	0.44	0.0828	1.1	1	0.4

$$\beta^* = 0.09, \quad \kappa = 0.42, \quad C_{mix} = 1.5,$$

$$\overline{u_i' u_j'} = \frac{\partial}{\partial x_j} \left(\nu_t \frac{\partial u_i}{\partial x_j} \right) + \frac{2}{3} k \delta_{ij} + a_{ij}^{(ex)} k \quad \text{and} \quad \nu_t = -\frac{1}{2} (\beta_1 + II_\Omega) \beta_6. \quad (9)$$

The anisotropic terms was defined

$$\begin{aligned} a_{ij}^{(ex)} = & \beta_3 \left(\Omega_{ik} \Omega_{kj} - \frac{1}{3} II_\Omega \delta_{ij} \right) + \beta_4 \left(S_{ik} \Omega_{kj} - \Omega_{ik} S_{kj} \right) \\ & + \beta_6 \left(S_{ik} \Omega_{kl} \Omega_{lj} + \Omega_{ik} \Omega_{kl} S_{lj} - II_\Omega S_{ij} - \frac{2}{3} IV \delta_{ij} \right) \\ & + \beta_9 \left(\Omega_{ik} S_{kl} \Omega_{lm} \Omega_{mj} + \Omega_{ik} \Omega_{kl} S_{lm} \Omega_{mj} \right) \end{aligned} \quad (10)$$

The strain-rate and vorticity tensor are defined as

$$S_{ij} = \frac{1}{2} \tau \left(\frac{\partial u_i}{\partial x_j} + \frac{\partial u_j}{\partial x_i} \right), \Omega_{ij} = \frac{1}{2} \tau \left(\frac{\partial u_i}{\partial x_j} - \frac{\partial u_j}{\partial x_i} \right) \quad (11)$$

and time scale is defined as

$$\tau = \max \left(\frac{1}{\beta^* \omega}, 6.0 \sqrt{\frac{\nu}{\beta^* k \omega}} \right). \quad (12)$$

The β coefficients are functions of invariants $II_S = S_{kl} S_{lk}$, $II_\Omega = \Omega_{kl} \Omega_{lk}$, $III_S = S_{kl} S_{lm} S_{mk}$, $IV = S_{kl} \Omega_{lm} \Omega_{mk}$ and $V = S_{kl} S_{lm} \Omega_{mn} \Omega_{nk}$. This coefficients are defined as $\beta_1 = -N(2N^2 - 7II_\Omega)/Q$, $\beta_3 = -12 IV/(NQ)$, $\beta_4 = -2(N^2 - 2II_\Omega)/Q$, $\beta_6 = -6N/Q$ and $\beta_9 = -6/Q$,

where

$$Q = \frac{5}{6} (N^2 - 2II_\Omega) (2N^2 - II_\Omega) \quad (13)$$

and

$$N \approx N_C + \frac{162 [IV^2 + (V - 0.5II_S II_\Omega) N_C^2]}{20N_C^4 (N_C - 0.5A'_3) - II_\Omega (10N_C^3 + 15A'_3 N_C^2) + 10A'_3 II_\Omega}. \quad (14)$$

The N_C and A'_3 are defined as

$$N_C = \frac{A'_3}{3} + \sqrt[3]{P_1 + \sqrt{P_2}} + \text{sign}(P_1 - \sqrt{P_2}) \sqrt[3]{|P_1 - \sqrt{P_2}|} \quad P_2 \geq 0, \quad (15)$$

$$N_C = \frac{A'_3}{3} + 2\sqrt[3]{P_1 - P_2} \cos \left(\frac{1}{3} \arccos \left(\frac{P_1}{\sqrt{P_1^2 - P_2}} \right) \right) \quad P_2 < 0, \quad (16)$$

$$P_1 = \left(\frac{A'_3}{27} + \frac{9}{20} II_S - \frac{2}{3} II_\Omega \right) A'_3, \quad P_2 = P_1^2 - \left(\frac{A'^2_3}{9} + \frac{9}{10} II_S + \frac{2}{3} II_\Omega \right)^3, \quad (17)$$

$$A'_3 = \frac{9}{5} + \frac{99}{20} \max(1 + \beta_1^{eq} II_S, 0) \quad \text{and} \quad \beta_1^{eq} = -\frac{6}{5} \frac{\frac{81}{20}}{\left(\frac{81}{20} \right)^2 - 2II_\Omega}. \quad (18)$$

We expected that this model give us better results than standard k – omega models.

3 DROPLETS MODEL

The Eulerian model was chosen for the description of the droplets model as it has been written in introduction. We have used following assumptions for the derivation of this model. The shape of droplet is a perfect sphere and the droplets are moving in the cloud. There is only a one diameter of drops in the cloud and it is moving by common velocity. The movement of droplets is affected only by aerodynamic (lift and drag), gravity and buoyancy forces. This forces affect the flow fields too. In this time There are not included a dispersion model and wall interaction model. The model is described by this system of PDE's.

$$\frac{\partial \alpha}{\partial t} + \frac{\partial \alpha}{\partial x_i} v_i = 0, \quad (19)$$

$$\frac{\partial v_i}{\partial t} + \frac{\partial v_i}{\partial x_j} v_j = f_i, \quad (20)$$

where the volume fraction α is defined as

$$\alpha = \frac{V_{water}}{V_{air}}. \quad (21)$$

The forces was chosen the following model

$$f_i = f_{G_i} + f_{L_i} + f_{D_i}, \quad (22)$$

$$f_{G_i} = g_i, f_{L_i} = -\frac{\rho_{air}}{\rho_{water}} g_i \text{ and } f_{D_i} = -\frac{3}{4} \frac{c_d}{d} \frac{\rho_{air}}{\rho_{water}} |v_i - u_i| (v_i - u_i). \quad (23)$$

The drag coefficient of sphere drop is described by this model

$$c_d = \left[\frac{1}{(\varphi_1 + \varphi_2)^{-1} + \varphi_3^{-1} + \varphi_4} \right] \frac{1}{10} \quad (24)$$

where

$$\varphi_1 = \left(\frac{24}{Re_K} \right)^{10} + \left(\frac{21}{Re_K^{0,67}} \right)^{10} + \left(\frac{4}{Re_K^{0,33}} \right)^{10} + (0,4)^{10}, \quad (25)$$

$$\varphi_2 = \frac{1}{(0,148 \cdot Re_K^{0,11})^{-10} + 0,5^{-10}} \quad (26)$$

$$\varphi_3 = \left(\frac{1,57 \cdot 10^8}{Re_K^{1,625}} \right)^{10} \text{ and } \varphi_4 = \frac{1}{(1,67 \cdot 10^{-17} Re_K^{2,63})^{-10} + 0,2^{-10}}. \quad (27)$$

The coupling coefficient is defined as

$$\xi = n \frac{m_{water}}{m_{air}} \quad (28)$$

If coefficient n is equal to 1 than we obtain two way coupled model and If it is equal to 0 than we obtain one way coupled model.

4 NUMERICAL RESULTS

For numerical solution was chosen an open source CFD code OpenFOAM in this time. This code will be implemented into own implicit code in the future time. A flat plate was chosen for testing of turbulent model and airfoil NACA 0012 and DLR body were chosen for testing of droplets model.

In the figure 1 you can see a friction coefficient on the flat plate. Following boundary conditions and physical properties were chosen for this test case. Velocity $u_\infty = 5.4ms^{-1}$, pressure $\tilde{p}_\infty = 0m^2s^{-2}$ and kinematic viscosity $\nu = 1.5 \cdot 10^{-5}m^2s^{-1}$. Boundary conditions of turbulent model were derived from intensity of turbulent field $Tu = 0.03$ and from the ratio between turbulent viscosity and kinematic viscosity $\nu/\nu_{t_\infty} = 0.001$.

In the figure 2 you can see comparison between streamlines of velocities and trajectories of droplets in the near of leading edge of profile. In the figure 3 you can see comparison between coupling and non-coupling model. In the figure 4 you can see a result on 3D geometry of DLR. For this simulation following boundary properties $u_\infty = v_\infty = 5.4ms^{-1}$ and $\alpha_\infty = 4.2 \cdot 10^{-6}$ were used.

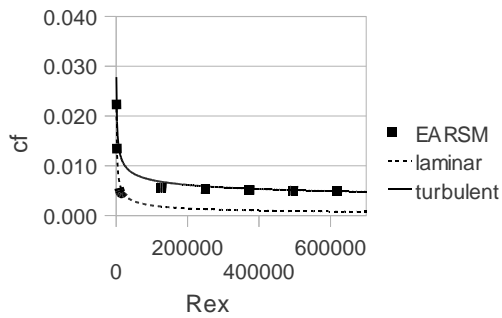


Fig. 1 Friction coefficient on the flat plate

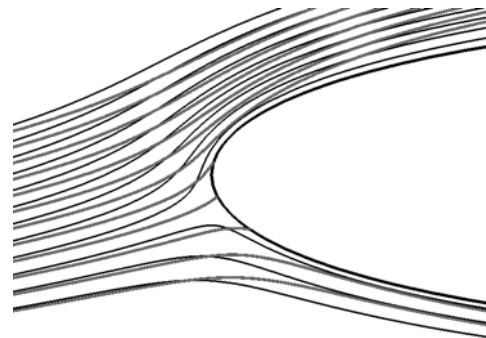


Fig. 2 Streamlines(black line) and trajectories (gray lines) in the near of leading edge

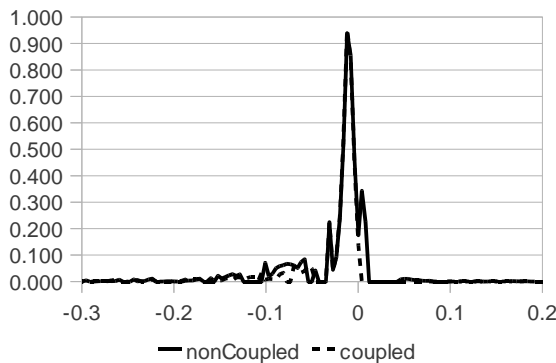


Fig. 3 Comparison of mass flux through the profile between non-coupled (continuous) and coupled(dash) droplets model

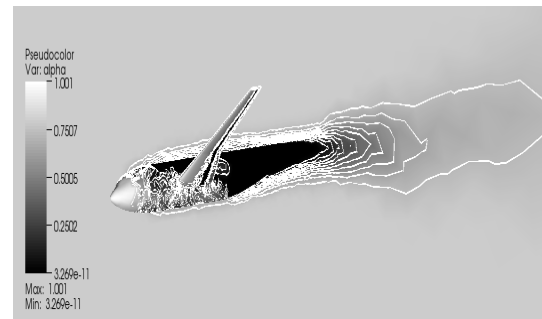


Fig. 4 Volume fraction in the near of DLR body

5 SUMMARY AND FUTURE WORK

The basic theory and the first results of two-way coupled Euler-Euler droplets solver were shown in this work. A big advantage of this model was shown in previous work [10] where the earlier version of this solver was compared with Euler-Lagrange approach. This approach is given us a lot of advantage especially in 3D simulation where significantly reduced CPU time.

In the future work I will target to next testing of turbulent model and of droplet model. The turbulent model will be extended to model of transition. The droplet model will be extended to model of interaction between droplets and thin fluid films to create a powerfull tool for simulation of ice growth on aircrafts.

REFERENCES

- [1] DVOŘÁK, R., KOZEL, K.: *Matematické modelování v aerodynamice*, CTU, Prague 1996
- [2] FOŘT, J., KOZEL, K., LOUDA, P., FÜRST, J.: *Numerické metody řešení problémů proudění*, CTU, Prague 2001
- [3] PŘÍHODA, J., LOUDA, P.: *Matematické modelování turbulentního proudění*, CTU, Prague 2007
- [4] HABASHI, W.: *Pacing In-flight Icing Simulation*,
http://zjw.public.iastate.edu/photos/stanford/HABASHI_ICING.pdf
- [5] ALMEDEIJ, J.: *Drag coefficient of flow around sphere: Matching asymptotically the wide trend*, Science, 16. 12. 2007
- [6] GEUZAINÉ, C., REMACLE, J.-F.: *Gmsh a three-dimensional finite element mesh generator with built-in pre- and post-processing facilities*, International Journal for Numerical Methods in Engineering, Volume 79, Issue 11, pages 1309-1331, 2009
- [7] JASAK, H.: *Error analysis and estimation for the finite volume method with applications to fluid flow*, Imperial College 1996
- [8] CROWE, C., SOMMERFIELD, M., TSUJI, Y.: *Multiphase Flows with droplets and particles*, CRC PRESS, 1998 http://www.geuz.org/gmsh/gmsh_paper_preprint.pdf

Acknowledgment: This work was supported by the Grant Agency of the Czech Technical University in Prague, grant No. SGS 10/243/0HK2/3T/12